Effect of the oxygen carrier ilmenite on NO<inf>X</inf> formation in chemical-looping combustion

Fuel Processing Technology 222 (2021) 106962

Contents lists available at ScienceDirect

Fuel Processing Technology

journal homepage: www.elsevier.com/locate/fuproc

Effect of the oxygen carrier ilmenite on NO_X formation in chemical-looping combustion

Stefan Mayrhuber [a], Fredrik Normann [b], Duygu Yilmaz [a,*], Henrik Leion [a]

[a] Department of Chemical and Biological Engineering, Division of Energy and Material, Chalmers University of Technology, SE-412 96 Gothenburg, Sweden
[b] Department of Energy and Environment, Division of Energy Technology, Chalmers University of Technology, SE-412 96 Gothenburg, Sweden

ARTICLE INFO

Keywords:
Chemical-looping combustion
Ilmenite
Nitrogen oxides
Perovskite catalyst
Oxygen carrier
Ammonia oxidation

ABSTRACT

The formation of NO_x from fuel-bound nitrogen is important for the design of chemical-looping combustion (CLC) power plants. This work studied to what extent NO and NH_3 reacts with the perovskite-like oxygen carrier ilmenite under conditions relevant to CLC. Based on mass balance calculations, N_2 was the major outlet N-species in all experiments. More NO was measured at lower temperatures and at a higher oxidation level of the oxygen carrier. The presence of syngas hindered the reduction of NO by ilmenite. There were significant differences between the two ilmenites studied with respect to N-species selectivity. Norwegian (rock) ilmenite reduced NO efficiently and showed a stable reaction behavior compared to Australian (sand) ilmenite. This could be attributed to the higher titanium content of Norwegian ilmenite.

1. Introduction

In chemical-looping combustion (CLC), the oxygen required for combustion is provided by an oxygen carrier (OC), resulting in a combustion gas without atmospheric nitrogen. Thus, CO_2 could be inherently concentrated in the flue gas and captured [1]. Usually, an OC is a metal oxide that can be oxidized and reduced at temperatures relevant to combustion. The OC circulates between two interconnected fluidized bed reactors, transporting air-bound oxygen from the air reactor to the fuel reactor [2,3].

In recent years, solid fuels (e.g. coal and biomass) are gaining in importance for CLC [2]. Solid fuels typically contain fuel-bound nitrogen compounds (1 to 2 wt-%) which are released mainly as NH_3 and HCN and are oxidized to nitrogen oxides (NO_x) or nitrogen during combustion, as shown in Fig. 1a [4]. For the design of CLC power plants and especially for carbon capture, formation of NO_x has to be considered [5].

Fig. 1b gives a simplified overview of the possible reaction paths for fuel-bound nitrogen (represented by NH_3). Catalytic decomposition of NH_3 occurs at temperatures above 400 °C, according to Reaction (1):

$$2\ NH_3 \rightleftharpoons N_2 + 3H_2 \qquad \Delta_r H^\circ_{298\,K} = +46.0\ \mathrm{kJ/mol_{NH_3}} \tag{1}$$

Since certain metal ions such as iron or nickel catalytically enhance the decomposition of NH_3 compared to sand, this reaction is probably important for CLC [7]. NO formation is controlled by heterogeneous reaction with the OC (Me_xO_y), as atmospheric oxygen is not present in the fuel reactor:

$$2NH_3 + 5Me_xO_y \rightleftharpoons 5Me_xO_{y-1} + 2NO + 3H_2O \tag{2}$$

For Fe_2O_3 as OC, the endothermic heat of reaction $\Delta_r H^\circ_{298\,K}$ is +373.4 $\mathrm{kJ/mol_{NH_3}}$. This reaction takes place at about 700 °C and only if the OC is sufficiently oxidized [7]. Other species such as NO_2 and N_2O are not released or only in very small quantities [8]. In contrast to normal combustion, no Zeldovich (thermal) NO_x and no Fenimore[1] (prompt) NO_x are produced because of moderate combustion temperatures (800 to 1000 °C) and due to the absence of hydrocarbons [10,11]. Already formed NO can be reduced to N_2 by NH_3 or syngas, as follows:

$$6\ NO + 4NH_3 \rightleftharpoons 5\ N_2 + 6H_2O \qquad \Delta_r H^\circ_{298\,K} = -301.5\ \mathrm{kJ/mol_{NO}} \tag{3}$$

$$2NO + CO + H_2 \rightleftharpoons N_2 + CO_2 + H_2O \qquad \Delta_r H^\circ_{298\,K} = -352.8\ \mathrm{kJ/mol_{NO}} \tag{4}$$

These gas-phase reactions can be catalytically promoted by the OC [7]. Certain OCs (e.g. Fe_3O_4 or ilmenite ($FeTiO_3$)), if sufficiently reduced, can also reduce NO through the following reaction:

$$2NO + 2Me_xO_{y-1} \rightleftharpoons N_2 + 2Me_xO_y \tag{5}$$

* Corresponding author.
E-mail address: duyguy@chalmers.se (D. Yilmaz).

[1] In the Fenimore mechanism, CH-radicals increase NO formation from N_2 especially in fuel-rich flames [9].

https://doi.org/10.1016/j.fuproc.2021.106962
Received 8 February 2021; Received in revised form 11 June 2021; Accepted 11 July 2021
Available online 16 July 2021

The heat of reaction $\Delta_r H^{\circ}_{298\,K}$ for the OC Fe_2O_3 is −330.3 kJ/mol_{NO}.

In this study, the behavior of the natural iron-titanium mineral *ilmenite* ($FeTiO_3$) as an OC was investigated. It is an attractive and inexpensive OC, has a high melting point, good fluidization properties and a long lifetime [12–14]. Therefore, ilmenite and other Fe-based compounds are used as OCs in many articles on CLC [7,13,15–23].

The structure of ilmenite is perovskite-like[2] (ABO_3) [26]. Here, the smaller cation (titanium) forms a three-dimensional network of octahedra with oxygen (TiO_6) and the larger cation (iron) is located between this network of octahedra [27,28]. Because of this structure, perovskite-like catalysts can adsorb and desorb NO_x, are not poisoned by SO_2 and H_2O, show hydrothermal stability and selective catalytic reduction (SCR) of NO [29,30]. Thus, many groups recommend perovskite-type catalysts for NO_x reduction (e.g. in diesel engines or power plants) [27,31–34].

This work follows up on several articles published in recent years on NO_x formation in CLC. Cheng et al. investigated catalytic decomposition and oxidation of NH_3 over ilmenite and the reduction of NO by reduced ilmenite and NH_3. In doing so, the influence of the NH_3 and syngas feed concentration on the N-species selectivity was examined [7]. The oxidation of NH_3 with copper oxide as OC was studied by Normann et al. Here, the influence of the syngas/NH_3 ratio, the ammonia gas fraction and ageing of the OC on the NO_x formation were investigated [6]. Wang et al. studied the conditions of an OC aided combustion in a laboratory-scale reactor. Among other things, the influence of different OCs and different air/fuel ratios on NO release were investigated. The used OCs were ilmenite, manganese ore and two oxide slags [35].

The aim of this study was to experimentally characterize the nitrogen chemistry in presence of the perovskite-like OC ilmenite. Especially, the effect of temperature and oxidation level of the OC on the amount of NO_x released were of interest. Experiments were conducted with two different ilmenites (Norwegian rock ilmenite and Australian sand ilmenite) to investigate possible differences in reactivity and stability, based on their elemental composition and structure.

2. Material and Methods

2.1. Oxygen carrier

The *Norwegian ilmenite* is a natural iron-titanium oxide supplied by Titania A/S. It is a *rock ilmenite*, because it is formed by crushing rocks containing ilmenite. In its original / reduced state, this ore consists of 65.5% $FeTiO_3$ (ilmenite), 14.8% Fe_2O_3 and 14% TiO_2. This OC has been used previously in a 100 kW_{th} CLC reactor system with fluidized bed for many hours. More detailed data on this ilmenite may be found elsewhere. [13,19,20]

The *Australian ilmenite* is a *sand ilmenite* mined from an Australian sand mine. It was also used as an OC by Cheng et al. [7]. Unlike to the ilmenite from Norway, this was previously used only in a laboratory reactor for about 35 cycles.

To obtain a good fluidization in the laboratory reactor, the particles of both ilmenites were sieved to a size interval 125–180 μm. The ilmenite powders were characterized by X-ray diffraction (Siemens™ D5000, Cu-Kα, 40 kV, 40 mA) in the range $2\Theta = 15 - 80^{\circ}$ with a step size of 0.01 and Scanning Electron Microscope (Zeiss™ LEO Ultra 55 FEG) for phase analysis and morphological characteristics, respectively. Quantitative phase analysis was performed via using RIR (reference intensity ratio) and supported by Rietveld Refinement technique.

The morphological characteristics of the Norwegian ilmenite ore can be seen in Fig. 2a. It has rocky morphology with sharp edges and randomly dispersed few hundred micrometer-sized distributions. In Fig. 2b, the Australian ilmenite is seen with smaller particle size than the Norwegian ilmenite. It shows rounder and sandier morphology.

2.2. Experimental

The experiments were conducted in a laboratory-scale fluidized-bed reactor, as illustrated in Fig. 3. This reactor consisted of a vertical quartz tube with an inner diameter d_i of 22 mm and a length of 820 mm. On a porous quartz plate, 15 g of an OC were placed 370 mm from the bottom of the reactor. The top of the reactor was filled with glass wool to trap gas-borne particles at the upper outlet of the laboratory reactor. An electrical furnace (ElectroHeat Sweden) heated the reactor externally. The temperature was measured by two K-type thermocouples (Pentronic; diameter: 3 mm). One thermocouple was placed 25 mm above the quartz plate with the OC and the other 5 mm below the OC. The specified reactor temperature of the various experiments ($T = 825^{\circ}C$ to 975 °C) always refers to the temperature-sensor above the quartz plate. A pressure gauge (Honeywell; frequency: 20 Hz) measured the pressure drop over time in the bed of solid particles to determine if a fluidized bed was present. The experiments were performed at atmospheric pressure. The reactor acted both as a fuel reactor and as an air reactor. This was done by alternately injecting reducing or oxidizing gas to the reactor via electromagnetic valves (Parker). The gas flow of each gas type (N_2, syngas, NH_3, etc.) was controlled with a mass flow controller (Brooks 5850 E Series). A total flow rate of 900 SmL/min guaranteed a bubbling fluidization of the OC. A heating band (Thermocoax Isopad GMBH) was used to keep the combustion gas warm and to avoid water condensation

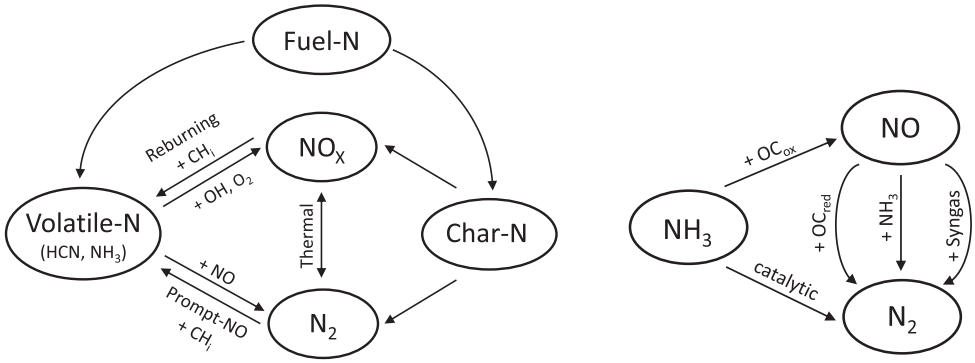

(a) Global mechanisms in normal combustion based on [6] (b) Possible reactions in CLC

Fig. 1. Reactions with nitrogen species in normal combustion (a) and in chemical-looping combustion (CLC) (b).

[2] In the perovskite structure (ABO_3), ionic radius of the B cation is permitted to vary only to a limited extent which called the tolerance factor. For the perovskite structure, this tolerance factor varies between 0.8 and 1, while in the ilmenite structure ($FeTiO_3$) it is less than 0.8. [24,25]

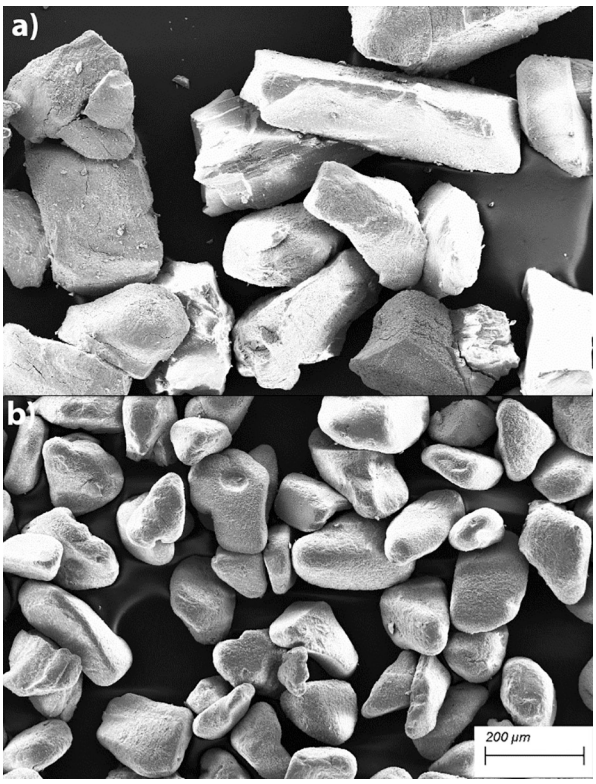

Fig. 2. SEM micrographs of ilmenites as raw materials.

in the tube. A detailed overview of the system can be found elsewhere. [36]

To analyze the gas concentration of the relevant compounds simultaneously, the gas flow was split in two streams one for the main gas analyzer and one for the NO_x analyzer. Before the gas flowed into the gas-analyzer, it was cooled down and dried (M&C Cooler ECP1000; BOO Instrument AB). The concentrations of O_2, CO and CO_2 were measured with a *Rosemount NGA 2000 Multi-Component Gas Analyzer* (Emerson Electric Company, Ferguson, USA). The gas analyzer was calibrated on a daily bases. A constant gas flow of approximately 400 SmL/min of the total flow was diverted for the NO_x analysis. NH_3 was captured in a 75 mmol/L solution of sulfuric acid (ammonia trap) which was cooled to 0 °C in an ice bath. The ammonia trap contained about 50 mL of diluted acid (H_2SO_4) which was replaced after each cycle. The sample was characterized by *ion chromatography* (ICS-900; DIONEX) to determine the amount of $(NH_3)_2SO_4$. The eluent used for the ion chromatography was a 20 mmol/L solution of methanesulfonic acid (CH_4O_3S). After the ammonia trap, the NH_3 free gas was dried with a drying agent (P_5O_{10}) to avoid interactions of moisture on the NO_x measurement. The gas concentrations of NO and NO_2 were measured by a *chemiluminescence analyzer* (CLD 700 EL ht.; ECO Physics BOO Instrument AB).

2.3. Procedure

One cycle consisted of 1) the oxidation phase (simulates the air reactor) and 2) the reduction phase (simulates the fuel reactor). Between the two operating phases, the reactor was inerted with nitrogen. Oxidation of the OC was carried out with a dilute oxygen stream (5 vol–% O_2 in N_2). In some experiments, the reduction phase was divided into short pulses of 10 s to prevent back mixing and to obtain a better resolution of the OC reduction process. Between pulses the reactor was inerted with N_2. Pulse experiments were performed with simultaneous syngas and NH_3 / NO, as shown in Fig. 4a, and pulses with only NH_3 / NO (syngas was introduced to reduce the OC to a certain level), as shown in Fig. 4b.

The test matrix for the experiments with Norwegian and Australian ilmenite and different gas mixtures (syngas, NO and NH_3) is shown in Table 1.

2.4. Data evaluation

The following set of parameters was used to evaluate the experiments:

Gas conversion γ_{CO} determines conversion of syngas to CO_2 and H_2O during the reduction of the OC. The gas conversion is a measure of the reactivity of the OC at different reduction levels or temperatures. Since the H_2 concentration at the exit was not measured, the completeness of the reduction was determined using the gas conversion of CO according to Eq. 6.

$$\gamma_{CO} = \frac{x_{CO_2}}{x_{CO_2} + x_{CO}} \tag{6}$$

Here, x_i is the mole fraction of component *i*. Hydrogen was assumed

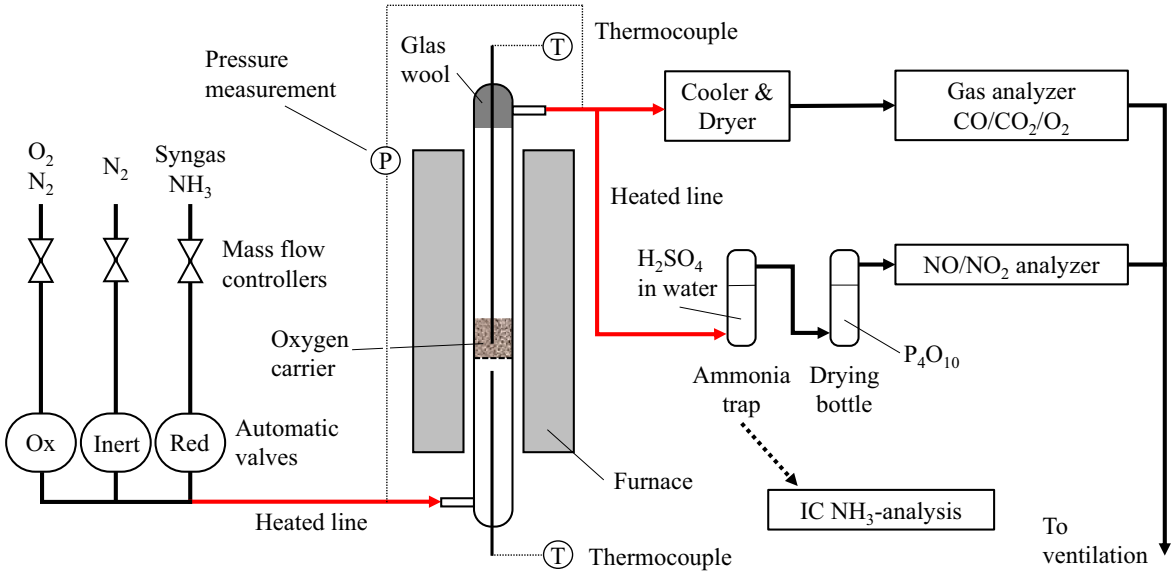

Fig. 3. Schematic of the experimental setup.

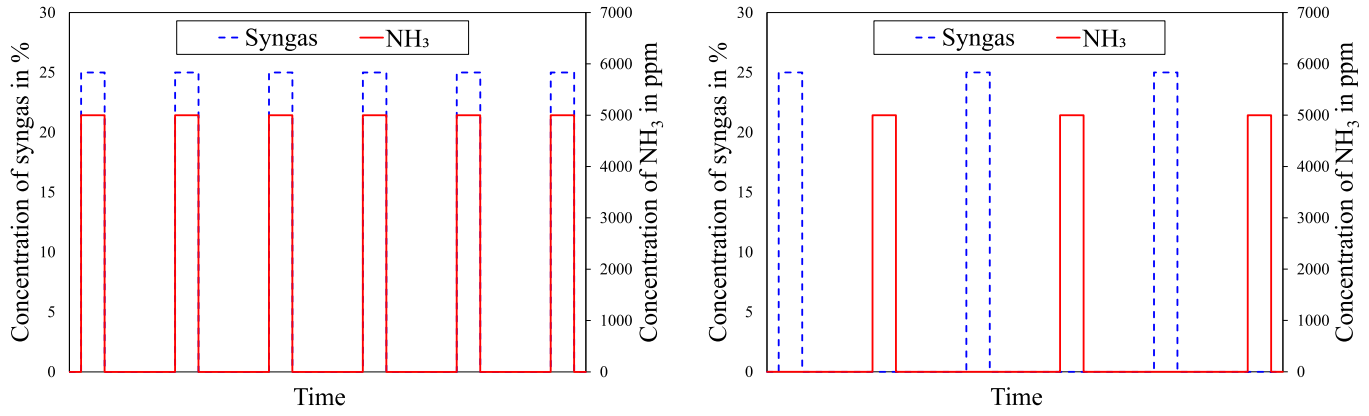

Fig. 4. Introduced reactants during reduction phase of pulse experiments.

Table 1
Test matrix for experiments with Norwegian ilmenite and Australian ilmenite.

Reduction type	Temperature	NH_3 fraction	NO fraction	Syngas fraction	Reduction time
–	[per-mode = symbol] °C	[per-mode = symbol] vol–%	[per-mode = symbol] vol–%	[per-mode = symbol] vol–%	[per-mode = symbol] s
Norwegian ilmenite					
continuous	825 / 875 / 925 / 975	0.5	0	25	160
pulses	825 / 875 / 925 / 975	0.5	0	0 / 25	16 pulses a 10
continuous	825 / 875 / 925 / 975	0.5	0	0	1200
pulses	825 / 875 / 925 / 975	0	0.25	0 / 25	17 pulses a 10
Australian ilmenite					
continuous	825 / 875 / 925 / 975	0.5	0	25	160
pulses	825 / 925	0.5	0	25	16 pulses a 10
continuous	825 / 875 / 925 / 975	1	0	0	1200

to be fully oxidized for all experiments. This is reasonable since hydrogen reacts faster than CO and CO conversion was high. For the experiments with only NH_3 (in N_2) as reducing gas, the conversion was calculated as follows:

$$\gamma_{NH_3} = 1 - \frac{n_{NH_3}}{n^0_{NH_3}} \tag{7}$$

Here, ${n_{NH_3}}^0$ was the amount of NH_3 introduced in the reactor during the reduction phase and n_{NH_3} are the moles of the NH_3 measured in the output.

Gas yield Y of NO is the ratio of the amount of NO in the outlet n_{NO} to the amount of NH_3 introduced into the reactor n^0_{NH3}, according to Eq. (8). As the gas stream was dried before the NO_x analyzer, the total exit flow $\dot{n}_{out}$ was depleted, which was considered in the calculation.

$$Y_{NO} = \frac{n_{NO}}{n^0_{NH_3}} = \frac{\int_{t_0}^{t_1} x_{NO}\,\dot{n}_{out}\,dt}{x^0_{NH_3}\,\dot{n}_{in}(t_1 - t_0)} \tag{8}$$

The formed n_{NO} was calculated by integration of the measured NO flow between the beginning of the OC reduction t_0 and the time t_1. The total mole flow $\dot{n}_{in}$ and the concentration of NH_3 ${x_{NH_3}}^0$ into the reactor were constant during the reduction of the OC.

Mass-based conversion ω is suitable to estimate the reduction level of the OC. This is defined as the ratio of the mass m of the OC to the mass m_{ox} of the fully oxidized OC (see Eq. (9)). A fully oxidized OC has a mass-based conversion ω of 1.

$$\omega = \frac{m}{m_{ox}} \tag{9}$$

Assuming a complete reaction, the mass-based conversion ω of the OC can be calculated from the concentrations of the injected gases x_i^0 using Eq. (10).

$$\omega(t_{red}) = 1 - \frac{\dot{n}_{in}\,\overline{M}_{O_2}}{m_{ox}}\left(0.5\,x^0_{syngas} + 0.75\,x^0_{NH_3} - 0.5\,x^0_{NO}\right)t_{red} \tag{10}$$

For a better comparison, the OC ilmenite was reduced to the same reduction level at each cycle ($\omega = 0.97$). t_{red} was the reduction time and $\overline{M}_{O_2}$ is the molar mass of oxygen.

3. Results

To study the influence of the OCs on the NO_X formation in CLC, the N-species selectivity and CO conversion were determined for different temperatures. Furthermore, the amount of NO released was investigated as a function of the mass-based conversions ω of ilmenite. It should be mentioned that no NO_2 was measured in any experiment.

3.1. Characterization of the nitrogen chemistry

Here, the nitrogen chemistry during the reduction of ilmenite by NH_3, NO and syngas was investigated by pulse experiments. Fig. 5 shows the gas yield Y of NO as a function of the mass-based conversion ω at different temperatures. No or only small amounts of NH_3 were measured in the ammonia trap, indicating that almost all introduced NH_3 was converted to N_2 or NO. This was similar to the results of Cheng et al. 2015 [7]. The amount of NO released decreased with an increasing temperature and with a decreasing mass-based conversion ω of the OC.

The experiments with syngas (see Fig. 5 left) showed a similar behavior. With respect to NO release, there was no significant difference whether NH_3 or NO was introduced into the reactor. Fig. 5a indicates that a fully oxidized ($\omega \approx 1$) Norwegian ilmenite at 825 °C can convert approximately 50% of the introduced NH_3 to NO. The question arises whether the oxidation of NH_3 to NO or the reduction of formed NO to N_2 was crucial for measured amount of NO. This is discussed in part 4. The experiment with syngas and NO showed that even a almost fully oxidized OC can reduce up to 50% of the introduced NO to N_2. In all experiments with syngas, NO was only traced if $\omega > 0.993$.

To investigate the influence of syngas on the release of NO, pulse experiments without syngas were also carried out (right figures). Without syngas, less NO was measured than with syngas. Here, NO was

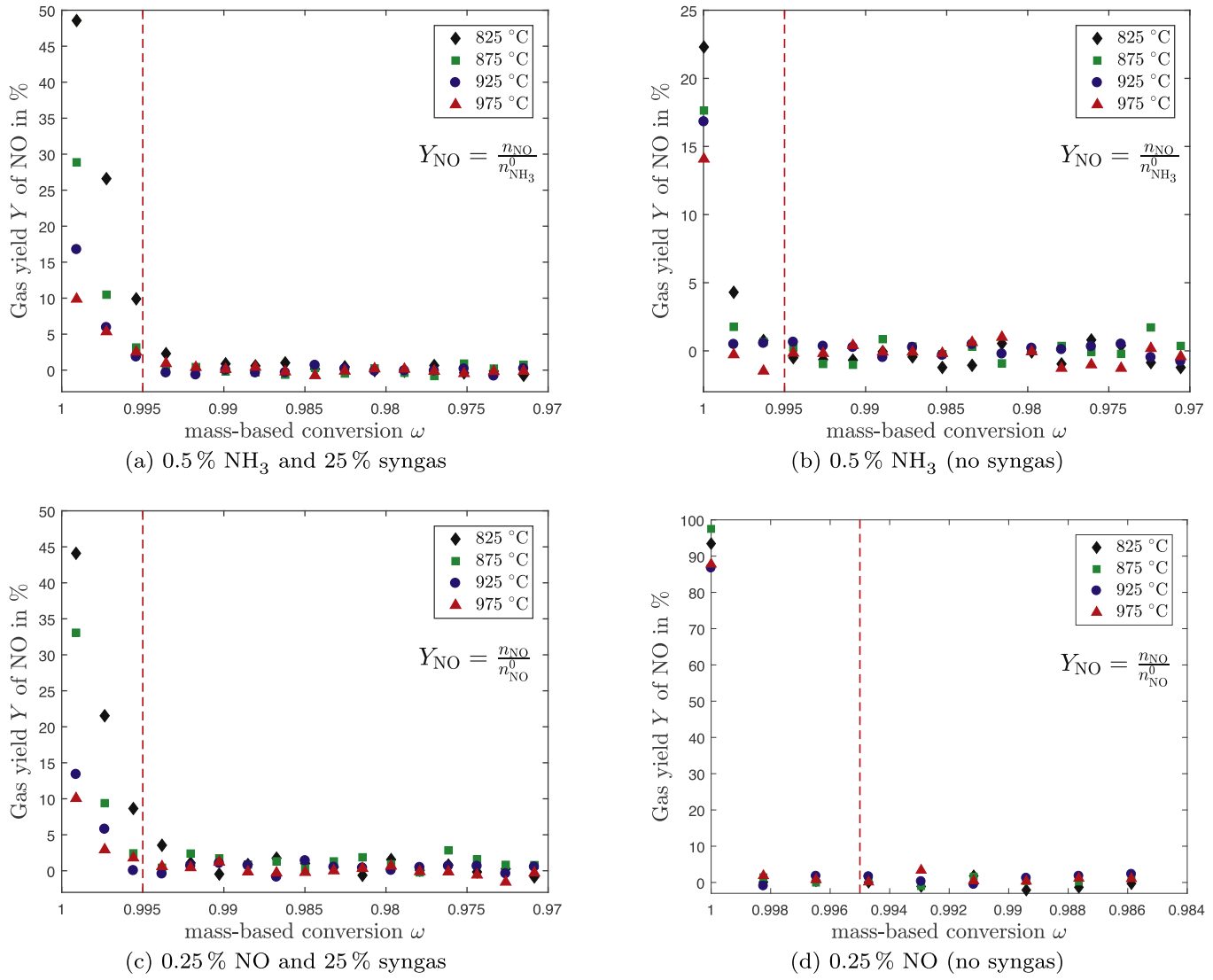

(a) 0.5 % NH_3 and 25 % syngas

(b) 0.5 % NH_3 (no syngas)

(c) 0.25 % NO and 25 % syngas

(d) 0.25 % NO (no syngas)

Fig. 5. Pulses with different gas mixtures as reducing gas at several temperatures; period of each pulse is 10 s; OC is Norwegian ilmenite; $\dot{V}_{flow} = 900\,SmL/min$; a red dashed line at $\omega = 0.995$ is added, to better compare the individual figures.

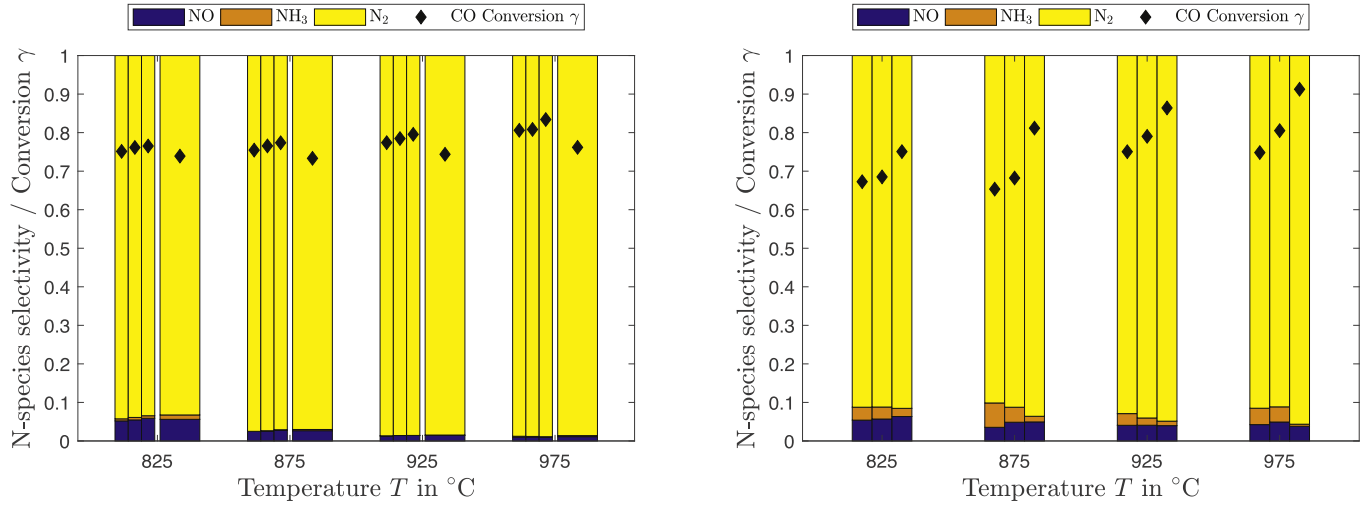

(a) Norwegian ilmenite

(b) Australian ilmenite

Fig. 6. N-species selectivity over an entire cycle at different temperatures; gas composition is 0.5% NH_3 and 25% syngas; reduction time of each cycle is 160 s; $\dot{V}_{flow} = 900\,SmL/min$; N_2 is given by difference. left: continuous reduction (thin bars) and reduction with pulses each 10 s (wide bars); right: continuous reduction.

only detected for an almost fully oxidized OC ($\omega > 0.997$). This was unexpected and was discussed in Section 4.

In Fig. 5d, only NO was introduced as reactant. NO was not oxidized like NH_3, but reduced by the reduced form of the OC. Only a fully oxidized OC cannot reduce NO, so a gas yield of approximately 100% was achieved. It can be assumed that NO can be efficiently reduced by Norwegian ilmenite, according to Reaction (5). Probably, this could be attributed to the perovskite-like structure of ilmenite. It should be mentioned that even the full oxidized OC did not oxidize NO to NO_2.

3.2. Comparison of different ilmenites

Since the Norwegian ilmenite has a different morphological character and a higher titanium content than the ilmenite from Australia, as shown in part 3.3, the reaction behavior of both ilmenites was compared. Fig. 6 illustrates the N-species selectivity over an entire reduction phase (with 25% syngas and 0.5% NH_3) for both ilmenites. Here, the OC was reduced to a mass-based conversion of $\omega = 0.972$. In the left figure with Norwegian ilmenite, three continuous reductions (thin bar) and a reduction with pulses (wide bars) are shown. It demonstrates that pulse experiments show similar patterns to continuous experiments with regard to the N-species selectivity Y and CO conversion γ.

Norwegian ilmenite had high cycle stability and high reactivity with syngas. Even after 45 h of experiments with this OC, gas conversions γ of CO between 85% and 90% were achieved when the OC was mostly oxidized ($\omega > 0.99$). In a 100 kW_{th} CLC reactor with Norwegian ilmenite, the gas conversion reached 83% and the ilmenite showed a lifetime of approximately 700 to 800 h [13]. More than 90% of the introduced NH_3 was converted to nitrogen and between 2 and 8% NO was released at each cycle. Only in the experiments at 825 °C certain residual amounts of NH_3 were visible. CO conversion was about 75% in all cases.

Australian ilmenite, in contrast to the experiments with Norwegian ilmenite, had not reached a cyclic stable state. CO conversion γ still rose over time and residual content of NH_3 decreased over time. Compared to Norwegian ilmenite, the temperature dependence of the amount of NO released was not as pronounced. Thus, more NO was detected at higher temperatures than with Norwegian ilmenite.

To better compare the two ilmenites, Fig. 7 shows pulse experiments with Australian ilmenite for two different temperatures under the same conditions as for Norwegian ilmenite in Fig. 5a. As expected, the comparison of Norwegian ilmenite (Fig. 5a) with Australian ilmenite (Fig. 7) revealed a similar reaction behavior. But more NO was formed at lower mass-based conversion ω for the Australian ilmenite. NO was measured up to $\omega > 0.990$ with Australian ilmenite.

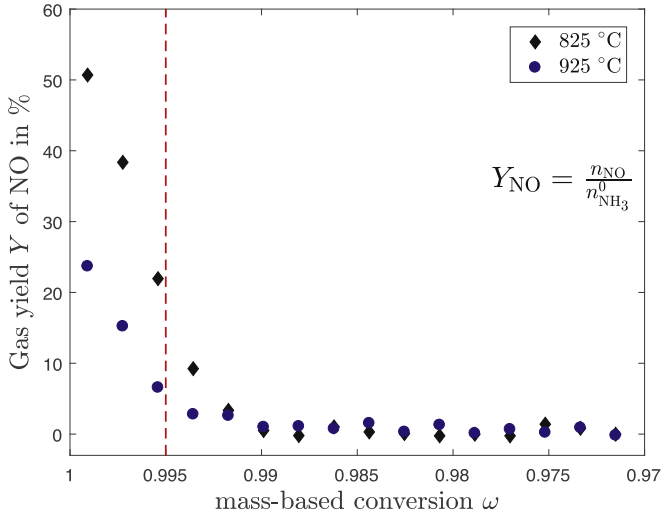

Fig. 7. Pulses with 0.5% NH_3 and 25% syngas at different temperatures; period of each pulse is 10 s; OC is Australian ilmenite; $\dot{V}_{flow} = 900\,SmL/min$; a red dashed line at $\omega = 0.995$ is added, to better compare the individual figures.

In Fig. 8, only NH_3 was introduced as reducing gas for 1200 s. Here, the specified mass-based conversion ω was calculated assuming that NH_3 was fully converted to nitrogen and water. Despite the long reduction time of 1200 s with NH_3 (and thus a much higher amount of NH_3 introduced compared to the other experiments) no significant amount of NH_3 was detectable neither for Norwegian ilmenite nor for Australian ilmenite.

Fig. 8a again shows that with Norwegian ilmenite, NO was formed only when the OC was almost completely oxidized ($\omega > 0.997$). In contrast, with Australian ilmenite, significant amounts of NO were still measured when the OC was reduced ($\omega < 0.988$). The amount of NO measured was about twice as large at high ω-values when comparing Australian ilmenite with Norwegian ilmenite. This can be attributed to the double amount of NH_3 introduced with Australian ilmenite.

In the article of Cheng et al. 2015 more than four times as much NO was measured with Australian ilmenite under similar reaction conditions [7]. Probably structural differences due to ageing of the Australian ilmenite could explain this, similar to the work of Cuadrat et al. 2012 [18]. To clarify whether there was an influence of ageing, Australian ilmenite was reduced with 1% NH_3 on three different days (see Fig. 8b). In the legend, in addition to the reaction temperature, the date and the corresponding cycle of the day were added. The general shape of all curves in Fig. 8b remains more or less the same. However, the amount of NO produced decreased over time. In particular, for a lower mass-based conversion ω (OC was more reduced), a large decrease in NO is recognizable. It seams the Australian ilmenite did not have such a stable reactivity over time as Norwegian ilmenite.

3.3. Characterization of the oxygen carriers

The morphological characteristics of the activated and used Norwegian and Australian ilmenite can be seen in Fig. 9. After the experiments, the Norwegian ilmenite was detected as corroded and fragmented into smaller particles. On the other hand, it can be seen that the Australian ilmenite preserved its morphology even after the experiments; however, cracks on the particles could be seen easily for both ilmenites. As the Norwegian ilmenite was previously used in a 100 kW_{th} CLC fluidized bed reactor for many hours, these difference on morphologies can be expected. As it can be seen in Table 2, the main phase of the Norwegian ilmenite, $FeTiO_3$ oxidized into Fe_5TiO_8 and Fe_2TiO_5 along Fe_2O_3 formation; while main phase of the Australian ilmenite, Fe_2TiO_5 dissociated into Fe_2O_3 and TiO_2. Elemental composition of both ilmenites from Table 3 also proved that the Norwegian ilmenite is richer about titanium content than the Australian ilmenite. This probably results with the formation of oxidized ilmenites rather than dissociation to Fe_2O_3 and TiO_2 during first seconds of the oxidation cycle, which makes the Norwegian ilmenite a good candidate for oxygen carrier [37,38]. In addition to this, as the Norwegian ilmenite has higher amount of $FeTiO_3$ and TiO_2 than the Australian ilmenite and coarser morphology, totally dissociation of ilmenites into Fe_2O_3 and TiO_2 takes more time compare to the Australian ilmenite, since the formation of ilmenites is most likely more probable rather than formation of Fe_2O_3 due to high TiO_2 content, which makes the Norwegian ilmenite more stable during cycles. However, it has been also known that particle strength increases when Fe:Ti ratio is increased in ilmenite, which affects the particle stability [39].

4. Discussion

The experiment with syngas and NH_3 (see Fig. 5a) suggested that up to 50% of the NH_3 can be converted to NO by ilmenite according to gas phase Reaction (2). According to Reaction (2), the formation of NO is endothermic, thus more NO would be expected to be formed at higher

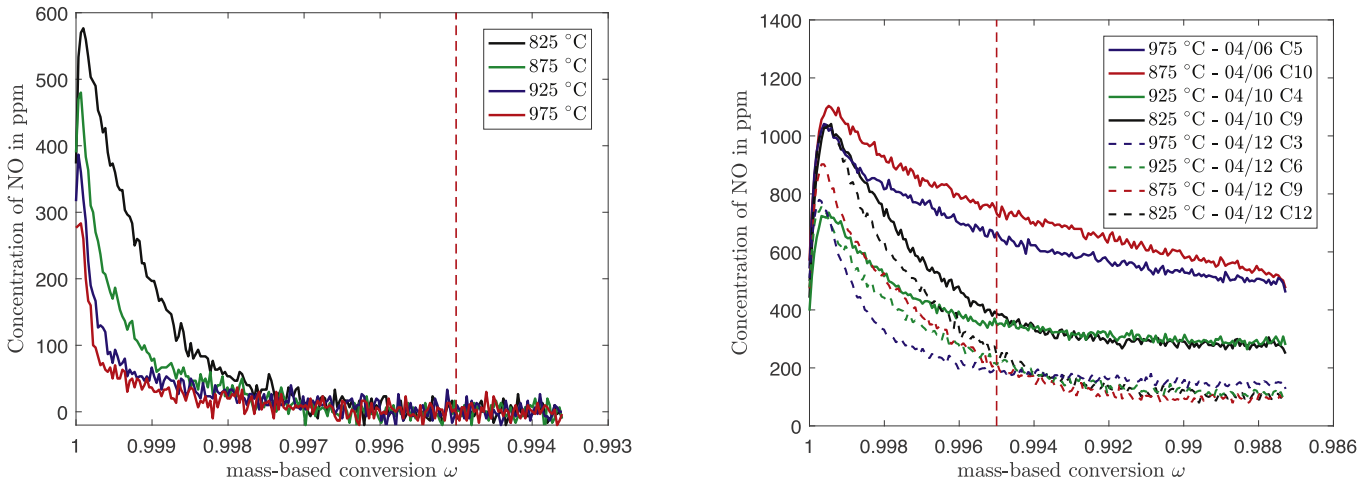

(a) Norwegian ilmenite; 0.5 % NH_3 as reducing gas

(b) Australian ilmenite; 1 % NH_3 as reducing gas

Fig. 8. Continuous reduction of ilmenite with NH_3 at different temperatures; reduction time is 1200 s; $\dot{V}_{flow} = 900\,SmL/min$; a red dashed line at $\omega = 0.995$ is added, to better compare the individual figures. With the Australian ilmenite two reduction cycles (date with cyclenumber) are conducted for each temperature.

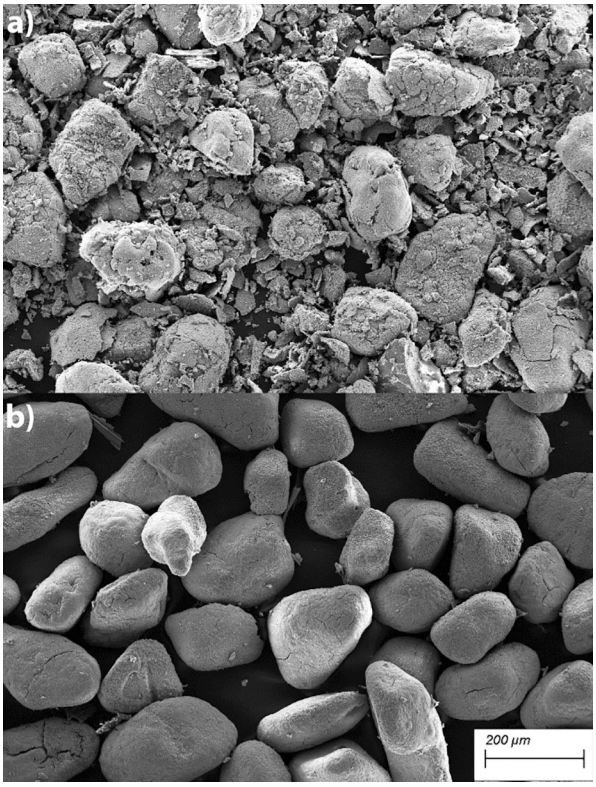

Fig. 9. SEM micrographs of ilmenites after being used in experiments.

temperatures, from both a thermodynamic and a kinetic point of view. However, since this was the opposite to the results in Fig. 5, not the formation of NO rather the reduction of formed NO to N_2 seemed to be crucial for the measured NO. For NO reduction the three Reactions (3), (5) and (4) form part 1 were discussed.

The pulse experiments with syngas (see Fig. 5a and c) showed that there was no influence on the gas yield Y of NO whether NH_3 or NO was fed. It seemed the reduction of NO with NH_3 according to Reaction (3) had a minor role on the total amount of NO. This could be due to the low concentration of NH_3 (0.5 vol–%) in the reactor.

A comparison of the experiments with and without syngas indicated that more NO was measured with syngas present in the reactor. This was

Table 2
Phase analysis of the Norwegian and the Australian ilmenite obtained by XRD both before and after used in experiments.

	Amount (wt-%)			
Compound	Australian ilmenite	Australian ilmenite - Used	Norwegian ilmenite	Norwegian ilmenite - Used
Fe_5TiO_8	–	–	–	8
Fe_2TiO_5	55	16	14	27
$FeTiO_3$	19	–	41	5
Fe_2O_3	14	59	23	41
TiO_2	7	18	15	13
Impurities	5	7	7	6

Table 3
Elemental composition of raw and used ilmenites in the experiments.

	Amount (wt-%)			
Element	Australian ilmenite	Australian ilmenite - Used	Norwegian ilmenite	Norwegian ilmenite - Used
Fe	46.22 ± 4.2	47.98 ± 2.2	31, 35 ± 1.7	32.67 ± 3.6
Ti	18.34 ± 3.2	12.15 ± 1.2	30.88 ± 1.2	22.46 ± 1.5
O	30.40 ± 5.1	36.36 ± 2.8	30.13 ± 3.4	39.43 ± 1.1
Impurities	5.04 ± 1.2	3.51 ± 1.4	7.64 ± 1.1	5.44 ± 3.8

unexpected, since from a thermodynamic point of view syngas should actually support the reduction of NO. Probably small amounts of CH-radicals were formed with syngas which promoted the formation of NO according to the *"Fenimore mechanism"*. Since of the low reaction temperatures it was unlikely that CH-radicals were formed from syngas in significant quantities [9,11]. To investigate the reduction of NO by syngas, an experiment was performed without an OC (see Appendix A). Despite there were 100 times more syngas than NO in the reactor syngas could only reduce between 30% and 50% of the introduced NO. This hinted that the effect of syngas was caused by the OC. More likely, there was a competition between syngas ($CO + H_2$) and NO for the OC. According to Becue et al. 2003, NO could be adsorbed and desorbed by the perovskite-like oxide ilmenite [26]. CO is similar in size and structure to NO and therefore might competes for the OC. In the experiments, there were 50 times more syngas (25 times more CO) in the reactor and therefore a much higher partial pressure of syngas (CO) which would improve the adsorption of syngas (CO) instead of NO by the OC.

The amount of released NO depended strongly on the OC conversion

ω. This indicated that of the three NO reduction Reactions (3), (5) and (4) the reduction of NO by the reduced OC according to Eq. (5) was pivotal. It was also shown in the pulse experiment with NO (see Fig. 5d), as NO was completely reduced here (except the OC was fully oxidized ($\omega = 1$)). This can be attributed to the catalytic effect of the perovskite-like structure of ilmenite [26,27].

5. Conclusion

A laboratory reactor with syngas (50% H_2 in CO) was used to simulate a CLC reaction with upstream gasification of a solid fuel. The evaluation focus was on the conversion of nitrogen present in the solid fuel, which was represented by small amounts of NH_3 or NO. The oxygen carrier was *ilmenite* (a titanium-iron ore) and the reaction process was evaluated with *pulse experiments* for better resolution.

In all experiments with NH_3 or NO introduced, the measured NO concentration in the reactor outlet decreased with increasing temperature. The gas yield Y of NO was more or less independent of whether NH_3 or NO was passed through the reactor and was increased in the presence of syngas. Syngas seemed to hinder the reduction of NO by the reduced ilmenite. NO was efficiently reduced to N_2 by the reduced form of ilmenite and no NO was formed at all when the mass-based conversion ω of ilmenite was above 0.99. Thus, NO reduction by ilmenite was most important for the NO concentration in the combustible gas.

There were significant differences between two different ilmenites (a Norwegian rock and an Australian sand ilmenite) in respect to N-species selectivity and gas conversion. In the experiments with the rock ilmenite from Norway, NH_3 was completely converted to NO or N_2. It was also very stable and showed conversions between 80% and 90% at 975 °C. A higher titanium concentration in the Norwegian ilmenite seemed to improve the reduction of NO and the cycle stability.

No NO_2 was measured in any experiment.

Declaration of Competing Interest

None.

Acknowledgments

This work was financially supported by the Swedish Research Council, Dnr 2016-05487.

Appendix A. Supplementary data

Supplementary data to this article can be found online at https://doi.org/10.1016/j.fuproc.2021.106962.

References

[1] A. Lyngfelt, B. Leckner, T. Mattisson, A fluidized-bed combustion process with inherent CO_2 separation; application of chemical-looping combustion, Chem. Eng. Sci. 56 (10) (2001) 3101–3113, https://doi.org/10.1016/S0009-2509(01)00007-0.
[2] J. Adanez, A. Abad, F. Garcia-Labiano, P. Gayan, L.F. de Diego, Progress in Chemical-Looping Combustion and Reforming technologies, Prog. Energy Combust. Sci. 38 (2) (2012) 215–282, https://doi.org/10.1016/j.pecs.2011.09.001.
[3] T. Mattisson, M. Keller, C. Linderholm, P. Moldenhauer, M. Rydén, H. Leion, A. Lyngfelt, Chemical-looping technologies using circulating fluidized bed systems: Status of development, Fuel Process. Technol. 172 (2018) 1–12, https://doi.org/10.1016/j.fuproc.2017.11.016.
[4] A. Lyngfelt, B. Leckner, A 1000 MWth boiler for chemical-looping combustion of solid fuels – Discussion of design and costs, Appl. Energy 157 (10) (2015) 475–487, https://doi.org/10.1016/j.apenergy.2015.04.057.
[5] F. Normann, K. Andersson, B. Leckner, F. Johnsson, Emission control of nitrogen oxides in the oxy-fuel process, Prog. Energy Combust. Sci. 35 (5) (2009) 385–397, https://doi.org/10.1016/j.pecs.2009.04.002.
[6] F. Normann, M. Cheng, D. Zhao, Z. Li, N. Cai, H. Leion, Oxidation of ammonia over a copper oxide-containing solid oxygen carrier with oxygen uncoupling capability, Combust. Flame 165 (2) (2016) 445–452, https://doi.org/10.1016/j.combustflame.2015.12.029.
[7] M. Cheng, F. Normann, D. Zhao, Z. Li, N. Cai, H. Leion, Oxidation of Ammonia by Ilmenite under Conditions Relevant to Chemical-Looping Combustion, Energy Fuel 29 (12) (2015) 8126–8134, https://doi.org/10.1021/acs.energyfuels.5b01939.
[8] T. Song, L. Shen, J. Xiao, D. Chen, H. Gu, S. Zhang, Nitrogen transfer of fuel-N in chemical looping combustion, Combustion and Flame 159 (3) (2012) 1286–1295, https://doi.org/10.1016/j.combustflame.2011.10.024.
[9] J. Santner, S.F. Ahmed, T. Farouk, F.L. Dryer, Computational Study of NO_x Formation at Conditions Relevant to Gas Turbine operation: part 1, Energy Fuel 30 (8) (2016) 6745–6755, https://doi.org/10.1021/acs.energyfuels.6b00420.
[10] J. Zhang, T. Ito, T. Okada, E. Oono, T. Suda, Improvement of NO_x formation model for pulverized coal combustion by increasing oxidation rate of HCN, Fuel 113 (2013) 697–706, https://doi.org/10.1016/j.fuel.2013.06.030.
[11] S.F. Ahmed, J. Santner, F.L. Dryer, B. Padak, T.I. Farouk, Computational Study of NO_x Formation at Conditions Relevant to Gas Turbine operation, part 2: NO_x in High Hydrogen Content fuel Combustion at Elevated pressure, Energy Fuel 30 (9) (2016) 7691–7703, https://doi.org/10.1021/acs.energyfuels.6b00421.
[12] H. Leion, A. Lyngfelt, M. Johansson, E. Jerndal, T. Mattisson, The use of ilmenite as an oxygen carrier in chemical-looping combustion, Chem. Eng. Res. Des. 86 (9) (2008) 1017–1026, https://doi.org/10.1016/j.cherd.2008.03.019.
[13] C. Linderholm, P. Knutsson, M. Schmitz, P. Markström, A. Lyngfelt, Material balances of carbon, sulfur, nitrogen and ilmenite in a 100 kW CLC reactor system, International Journal of Greenhouse Gas Control 27 (2014) 188–202, https://doi.org/10.1016/j.ijggc.2014.05.001.
[14] T. Mendiara, P. Gayán, A. Abad, F. García-Labiano, L.F. de Diego, J. Adánez, Characterization for disposal of Fe-based oxygen carriers from a CLC unit burning coal, Fuel Process. Technol. 138 (2015) 750–757, https://doi.org/10.1016/j.fuproc.2015.07.019.
[15] Z. Sun, D.Y. Lu, R.W. Hughes, D. Filippou, O_2 uncoupling behaviour of ilmenite and manganese-modified ilmenite as oxygen carriers, Fuel Process. Technol. 169 (2018) 15–23, https://doi.org/10.1016/j.fuproc.2017.08.025.
[16] D. Yamaguchi, L. Tang, J. Orellana, T.D. Hadley, S. Bhattacharya, K.-S. Lim, Characterisation of Australian ilmenite oxygen carrier during chemical looping combustion of Victorian brown coal, Fuel Process. Technol. 213 (10) (2021) 106669, https://doi.org/10.1016/j.fuproc.2020.106669.
[17] B. Tsedenbal, N. Kannari, K. Sato, H. Abe, H. Shirai, T. Takarada, Reforming of coal volatiles over ilmenite ore, Fuel Process. Technol. 192 (2019) 96–104, https://doi.org/10.1016/j.fuproc.2019.04.024.
[18] A. Cuadrat, A. Abad, J. Adánez, L.F. de Diego, F. García-Labiano, P. Gayán, Behavior of ilmenite as oxygen carrier in chemical-looping combustion, Fuel Process. Technol. 94 (1) (2012) 101–112, https://doi.org/10.1016/j.fuproc.2011.10.020.
[19] P. Knutsson, C. Linderholm, Characterization of ilmenite used as oxygen carrier in a 100 kW chemical-looping combustor for solid fuels, Appl. Energy 157 (2) (2015) 368–373, https://doi.org/10.1016/j.apenergy.2015.05.122.
[20] A. Lyngfelt, P. Markström, C. Linderholm, Chemical-Looping Combustion of Solid Fuels – Operational Experiences in 100 kW dual Circulating Fluidized Bed System, Energy Procedia 37 (2013) 608–617, https://doi.org/10.1016/j.egypro.2013.05.148.
[21] A. Abad, T. Mendiara, M.T. Izquierdo, L.F. de Diego, F. García-Labiano, P. Gayán, J. Adánez, Evaluation of the redox capability of manganese-titanium mixed oxides for thermochemical energy storage and chemical looping processes, Fuel Process. Technol. 211 (5) (2021) 106579, https://doi.org/10.1016/j.fuproc.2020.106579.
[22] R. Pérez-Vega, A. Abad, P. Gayán, F. García-Labiano, M.T. Izquierdo, L.F. de Diego, J. Adánez, Coal combustion via Chemical Looping assisted by Oxygen Uncoupling with a manganese-iron mixed oxide doped with titanium, Fuel Process. Technol. 197 (2) (2020) 106184, https://doi.org/10.1016/j.fuproc.2019.106184.
[23] Y. Zheng, L. Zhao, Y. Wang, Y. Wang, H. Wang, Y. Wang, L. Jiang, X. Zhu, Y. Wei, K. Li, Enhanced activity of $La_{1-x}MnCu_xO_3$ perovskite oxides for chemical looping steam methane reforming, Fuel Process. Technol. 215 (2021) 106744, https://doi.org/10.1016/j.fuproc.2021.106744.
[24] V.M. Goldschmidt (Ed.), Die Gesetze der Krystallochemie Vol. 14, 1926, https://doi.org/10.1007/BF01507527.
[25] A.F. Wells, Structural Inorganic Chemistry, 5th Edition, Oxford Classic Texts in the Physical Sciences, Oxford Univ Press, Oxford, 2012.
[26] T. Becue, K. Malefant, Method of removing nitrogen oxides using an ilmenite material, U.S. Patent 6,616,904 (2003).
[27] M. Jabłońska, R. Palkovits, Perovskite-based catalysts for the control of nitrogen oxide emissions from diesel engines, Catalysis Science & Technology 9 (9) (2019) 2057–2077, https://doi.org/10.1039/C8CY02458H.
[28] A.F. Holleman, E. Wiberg, Lehrbuch der anorganischen Chemie, 81st edition, de Gruyter, Berlin, 1976.
[29] D. Wang, Y. Peng, Q. Yang, S. Xiong, J. Li, J. Crittenden, Performance of modified $La_xSr_{1-x}MnO_3$ perovskite catalysts for NH_3 oxidation: TPD, DFT, and Kinetic Studies, Environmental science & technology 52 (13) (2018) 7443–7449, https://doi.org/10.1021/acs.est.8b01352.
[30] F. Liu, H. He, C. Zhang, Novel Iron Titanate Catalyst for the Selective Catalytic Reduction of NO with NH3 in the Medium Temperature Range, Chemical Communications (Cambridge, England) 17, 2008, pp. 2043–2045, https://doi.org/10.1039/b800143j.
[31] J.A. Onrubia-Calvo, B. Pereda-Ayo, J.R. González-Velasco, Perovskite-based Catalysts as Efficient, durable, and Economical NO_x Storage and Reduction Systems, Catalysts 10 (2) (2020) 208, https://doi.org/10.3390/catal10020208.
[32] Z. Li, M. Meng, Q. Li, Y. Xie, T. Hu, J. Zhang, Fe-substituted nanometric $La_{0.9}K_{0.1}co_{1-x}Fe_xO_{3-\delta}$ perovskite catalysts used for soot combustion, NO_x storage and simultaneous catalytic removal of soot and NO_x, Chem. Eng. J. 164 (1) (2010) 98–105, https://doi.org/10.1016/j.cej.2010.08.036.

[33] L. Han, S. Cai, M. Gao, J.-Y. Hasegawa, P. Wang, J. Zhang, L. Shi, D. Zhang, Selective Catalytic Reduction of NO_x with NH_3 by using Novel Catalysts: State of the Art and Future prospects, Chem. Rev. 119 (19) (2019) 10916–10976, https://doi.org/10.1021/acs.chemrev.9b00202.

[34] H. Wang, J. Liu, Z. Zhao, Y. Wei, C. Xu, Comparative study of nanometric Co-, Mn- and Fe-based perovskite-type complex oxide catalysts for the simultaneous elimination of soot and NO_x from diesel engine exhaust, Catal. Today 184 (1) (2012) 288–300, https://doi.org/10.1016/j.cattod.2012.01.005.

[35] P. Wang, H. Leion, H. Yang, Oxygen-Carrier-aided Combustion in a Bench-Scale Fluidized Bed, Energy Fuel 31 (6) (2017) 6463–6471, https://doi.org/10.1021/acs.energyfuels.7b00197.

[36] H. Leion, V. Frick, F. Hildor, Experimental method and setup for laboratory fluidized bed reactor testing, Energies 11 (10) (2018) 2505, https://doi.org/10.3390/en11102505.

[37] A. Abad, J. Adánez, A. Cuadrat, F. García-Labiano, P. Gayán, L.F. de Diego, Kinetics of redox reactions of ilmenite for chemical-looping combustion, Chem. Eng. Sci. 66 (4) (2011) 689–702, https://doi.org/10.1016/j.ces.2010.11.010.

[38] J. Nell, An overview of the phase-chemistry involved in the production of high-titanium slag from ilmenite feedstock, J. South African Inst. Min. Metal. (South Africa) 100 (2000) 35–44.

[39] M.M. Azis, E. Jerndal, H. Leion, T. Mattisson, A. Lyngfelt, On the evaluation of synthetic and natural ilmenite using syngas as fuel in chemical-looping combustion (CLC), Chem. Eng. Res. Des. 88 (11) (2010) 1505–1514, https://doi.org/10.1016/j.cherd.2010.03.006.